RESEARCH

Revisitation of imaging features of skull base chondrosarcoma in comparison to chordoma

Hirotaka Hasegawa[1] · Masahiro Shin[1,3] · Ryoko Niwa[1] · Satoshi Koizumi[1] · Shoko Yoshimoto[1] · Naoyuki Shono[1] ·
Yuki Shinya[1] · Hirokazu Takami[1] · Shota Tanaka[1] · Motoyuki Umekawa[1] · Shiori Amemiya[2] · Taichi Kin[1] ·
Nobuhito Saito[1]

Abstract

Purpose Pre-surgical diagnosis of skull base chondrosarcoma (SBC) is often challenging due to the resemblance to chordoma. The goal of this study was to develop an optimal method for predicting SBC diagnosis.

Methods This retrospective study included patients with histologically diagnosed SBC and skull base chordoma. Their clinical and radiologic features were compared, and the predictive factors of SBC were examined.

Results Forty-one patients with SBC and 41 with chordoma were included. Most SBCs exhibited hypointensity (25, 64.1%) or isointensity (12, 30.8%) on T1-weighted images, and hyperintensity (34, 87.1%) or mixed intensity (5, 12.8%) on T2-weighted images. MRI contrast enhancement was usually avid or fair (89.7%) with "arabesque"-like pattern (41.0%). The lateral/para-midline location was more common in SBC than in chordoma (85.4% vs. 9.8%; $P < 0.01$), while midline SBCs (14.6%) were also possible. Multivariate analysis demonstrated that higher apparent diffusion coefficient (ADC) value (unit odds ratio 1.01; 95% confidence interval 1.00–1.02; $P < 0.01$) was associated with an SBC diagnosis. An ADC value of $\geq 1750 \times 10^{-6}$ mm^2/s demonstrated a strong association with an SBC diagnosis (odds ratio 5.89×10^2; 95% confidence interval 51.0–6.80×10^3; $P < 0.01$) and yielded a sensitivity of 93.9%, specificity of 97.4%, positive predictive value of 96.9%, and negative predictive value of 95.0%.

Conclusion The ADC-based method is helpful in distinguishing SBC from chordoma and readily applicable in clinical practice. The prediction accuracy increases when other characteristics of SBC, such as non-midline location and arabesque-like enhancement, are considered together.

Keywords Apparent diffusion coefficient · Chondrosarcoma · Chordoma · Differential diagnosis · Magnetic resonance imaging · Radiologic features · Skull base

Introduction

Chondrosarcomas are rare malignant neoplasms of cartilage tissues that can develop in the skeletal system. Skull base chondrosarcomas (SBCs) are a rare subtype of chondrosarcoma, accounting for less than 10% of all chondrosarcomas and 0.15% of all intracranial tumors [1]. Accurate radiologic diagnosis is essential for elaborating tailored surgical strategies and subsequent treatment plans, balancing invasiveness and functional preservation. However, owing to the rarity of SBC and the presence of other tumors that can mimic SBC, physicians often encounter a diagnostic conundrum.

Several articles have reported detailed radiologic features of SBC; SBCs typically appear isointense or hypointense on T1-weighted images (T1WI) and hyperintense on T2-weighted images (T2WI) with avid contrast enhancement [2–5]. However, accurate preoperative diagnosis of SBC may be challenging for the following reasons. First, SBCs are mostly located in ventrolateral skull base, in which several other skull base tumors can arise. Second, surgeons sometimes encounter atypical-looking SBCs, such

✉ Hirotaka Hasegawa
  hasegawah-nsu@h.u-tokyo.ac.jp

1 Department of Neurosurgery, The University of Tokyo, 7-3-1 Hongo, Bunkyo, Tokyo 1138655, Japan

2 Department of Radiology, The University of Tokyo, Bunkyo, Tokyo, Japan

3 Department of Neurosurgery, Teikyo University, Itabashi, Tokyo, Japan

as centrally located SBCs and SBCs with minimal enhancement. Third, there remains a paucity of imaging features for other supportive imaging modalities, such as positron-emission tomography. In particular, chordomas are often indistinguishable from SBCs since they have several common radiologic features [4, 6, 7]. In the recent literature, radiomics analysis is reported to provide better diagnostic accuracy [8], but it remains too complicated to be widely used in clinical practice. Alternatively, diffusion-weighted imaging may be a promising tool for the differential diagnosis [9, 10].

Recent studies highlight significant biological differences between SBCs and chordomas; in general, better prognosis is expected and thus a less aggressive, functional preservation-oriented surgical strategy is recommended in SBCs, while more intensive, marginal resection is advocated for chordomas [11–15]. To create a tailored surgical strategy according to tumor histology and to explain the associated risk and prognosis to patients, accurate presurgical diagnosis is invaluable. The goal of the present study was to describe the detailed radiologic features of SBCs and to make comparisons with chordomas, creating a useful method in distinguishing SBCs from chordomas.

Methods

Patient selection

The study was approved by the institutional review board (IRB#2231). Written informed consent was obtained from all the study participants. This study adhered to the STROBE guideline [16]. Clinical and radiologic data of patients with histologically diagnosed SBC between 2002 and 2021 were retrospectively collected from hospital medical records and image databases. For comparison purposes, consecutive patients who had a new histological diagnosis of skull base chordoma before 2021 were retrospectively reviewed and collected until the same number of patients with SBC were obtained. To focus on pre-surgical diagnosis, only those in whom digital radiologic data before initial intervention were available for review were included since surgeries/radiotherapies and subsequent recurrences could alter imaging features, including location, signal intensities (SIs), and enhancement patterns.

Data acquisition

The patients' baseline characteristics were collected from the medical records. MRIs were performed using 1.5- or 3.0-T machines (1.5-T field strength, SIGNA Excite, GE Healthcare, IL, US; MAGNETOM Vision and MAGNETOM Avanto, Siemens Healthineers, Erlangen, Germany; 3.0-T

field strength, SIGNA HDxt and SIGNA Premier, GE Healthcare; Skyra, Siemens Healthineers; Ingenia CX, Philips, Amsterdam, Netherlands) with the following acquisition parameters: T1WI, repetition time (TR)/echo time (TE) 400–520/2.26–15 ms at 5-mm thickness for Siemens machines, 659/8 ms at 5-mm thickness for Philips machine, and TR/TE 400–640/8.4–11 ms at 3–5-mm thickness for GE machines; T2WI, TR/TE 3200–4260/84–105 ms at 3–5-mm thickness for Siemens machines, TR/TE 4160–4163/90 ms at 3-mm thickness for Philips machine, and TR/TE 4000–5420/78.8–98.2 ms at 3–5-mm thickness for GE machines; DWI, TR/TE 4400–4750/81–86 ms at 5-mm thickness, $b = 1000$ s/mm^2 for Siemens machines, TR/TE 4841/66 ms at 5-mm thickness, $b = 1000$ s/mm^2 for Philips machine, and TR/TE 4500–7800/59.3–74 ms at 5-mm thickness, $b = 1000$ s/mm^2 for GE machines; contrasted T1WI, TR/TE 18–24/2.3–3.4 ms at 0.4–0.8-mm thickness for Siemens machines, TR/TE 20/3.8–3.9 ms at 0.8-mm thickness for Philips machine, and TR/TE 20–24/2.2–3.1 ms at 0.8–2-mm thickness for GE machines. Apparent diffusion coefficient (ADC) maps were generated by built-in software provided by the MRI scanner vendors. SIs on T1WI and T2WI were measured by two co-authors who were blinded to the patient details using an ellipsoid-shaped region of interest, which was placed around the center of the tumor and adjusted as large as possible but not exceeding the tumor matrix, excluding regions of intratumoral calcification and hemorrhage as well as regions of entrapment of mucus (mucocele). Since SIs on T1- and T2-weighted images are relative values influenced by acquisition conditions and other factors, the SI ratio ([SI of the tumor]/[SI of the white matter]) was calculated for standardization. ADC values, which are absolute values in contrast to T1WI- and T2WI-SIs, were also measured using a similar method. Using gadolinium-enhanced T1WI, the degree and patterns of enhancement were evaluated separately; the degree was graded as "avid" if the enhancement was similar to the nasal mucosa, "fair" if it was less than the nasal mucosa but similar to muscle tissues, or "little" if it was less than the muscle tissues (Fig. 1A). The patterns of enhanced internal structures were classified as "homogenous" or "heterogenous"; in particular, "arabesque" was recorded if a characteristic "septal or ring-and-arc enhancement" [17, 18] was seen, forming an arabesque-like pattern (Fig. 1B). The tumor volume was estimated using the simplified formula for volume of ellipsoid: abc/2 [19]. Origins of SBCs were estimated based on the "centerpoint" of the tumor; a synchondrosis that was the closest to the tumor's center point was considered as the origin (Fig. 1C) [4]. When 18F-fluorodeoxyglucose PET data were available, lesion to normal tissue ratios (L/N ratios), which were calculated using the contralateral cerebral cortex or cerebellum and generally preferred to standardized uptake values for brain lesions [20], were recorded. The presence
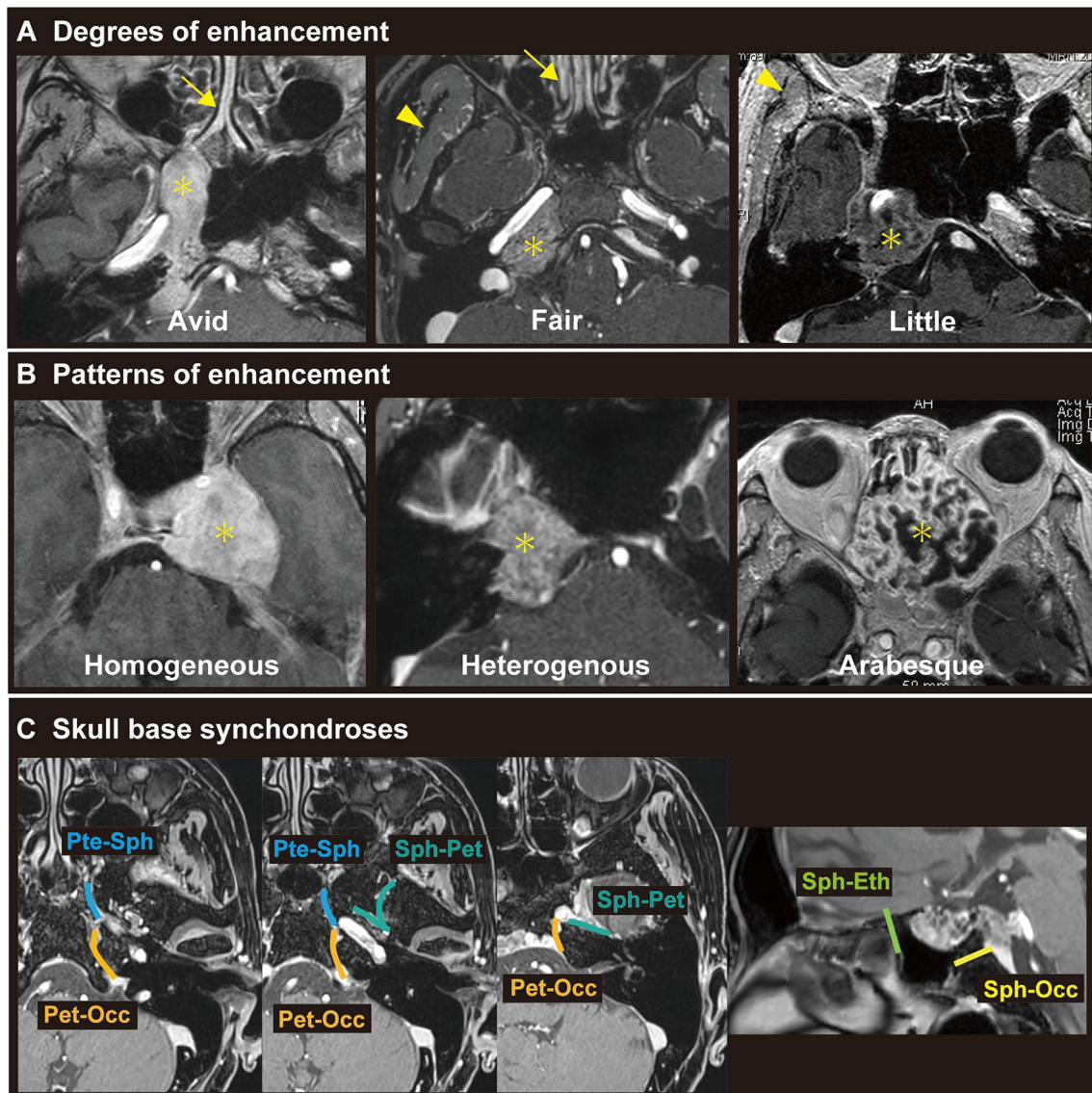
Fig. 1 Examples of degrees (**A**) and patterns (**B**) of contrast enhancement and skull base synchondroses (**C**). Yellow asterisk, tumor; yellow arrow, nasal mucosa; yellow arrowhead, muscle tissues. *Pet-Occ* petro-occipital synchondrosis, *Sph-Sph* pterygo-sphenoidal synchondrosis, *Sph-Eth* spheno-ethmoidal synchondrosis, *Sph-Occ* spheno-occipital synchondrosis, *Sph-Pet* spheno-petrosal synchondrosis

of intratumoral calcification and associated bone erosion, which are often indistinguishable, was evaluated using CT images.

Statistical analysis

Differences of the baseline characteristics and radiologic features between SBC and chordoma were tested using Fisher's exact test (categorical variables) and Mann–Whitney U test (continuous variables). Logistic regression analysis was used to examine the clinical and radiologic factors associated with the diagnosis of SBC. Multivariate analysis was performed using factors that were significant in the bivariate analysis.

Finally, using the factors that had a significant association with the diagnosis of SBC, a prediction method for SBC diagnosis was developed. Receiver operating characteristic (ROC) analysis was performed to determine the cutoff value that maximized the diagnostic potential based on the Youden index [21]. A P value of < 0.05 was considered significant in all statistical analyses. All statistical analyses were performed using JMP Pro 16.0 (SAS Institute, NC, USA).

Results

Overview of the cohorts

Among 55 patients with a histological diagnosis of SBC, 41 were included in the study after excluding 16 patients in whom imaging data before initial intervention were not available. There were five (12.2%) grade I, 31 (75.6%) grade II, and two (4.9%) grade III conventional SBCs, one (2.4%) myxoid subtype, one (2.4%) mesenchymal subtype, and one (2.4%) unspecified subtype. The representative cases are illustrated in Figs. 2 and 3. For comparison, 41 consecutive patients with chordomas (30 conventional, 10 chondroid, and one dedifferentiated) were included in the study. The clinical and radiologic features of the patients are summarized in Table 1; compared to chordoma, no factors were significantly associated with SBC, although there were the following tendencies: slightly more female predominance (63.4% vs. 51.2%, P = 0.27), slightly younger age at presentation (41.0 years vs. 48.0 years, P = 0.24), more frequent occurrence of headache/neck pain (14.6% vs. 4.9%, P = 0.26).

Radiologic features

Most SBCs exhibited hypointensity (27, 65.9%) or isointensity (12, 29.3%) on T1WI, and hyperintensity (35, 85.4%) or hyperintensity mixed with smaller hypointense areas (6, 14.6%) on T2WI. Regarding the patterns of enhancement on MRI, the arabesque pattern (18, 43.9%) was the most common, followed by the heterogeneous (14, 34.1%) and homogenous (9, 22.0%) patterns. Avid enhancement was the most common (23, 56.1%), followed by fair (14, 34.2%) and little (4, 9.8%) enhancement.

Data on T1SI- and T2SI-ratios was available in all patients, whereas ADC value was available in 32 SBC and 39 chordoma patients. Compared to chordomas, SBCs were significantly associated with a higher T2SI-ratio (P < 0.01) and ADC value (P < 0.01) (Table 1). While only a few chordomas exhibited an arabesque enhancement pattern (2, 4.9%), the majority of them had either heterogeneous (21, 51.2%) or homogenous (15, 36.6%) enhancement. Massive necrosis was seen in two patients (2.4%), while small areas of necrosis in background homogenous enhancement were seen in 2 (4.9%). Regarding the intensity of enhancement, little (16, 39.0%) enhancement was
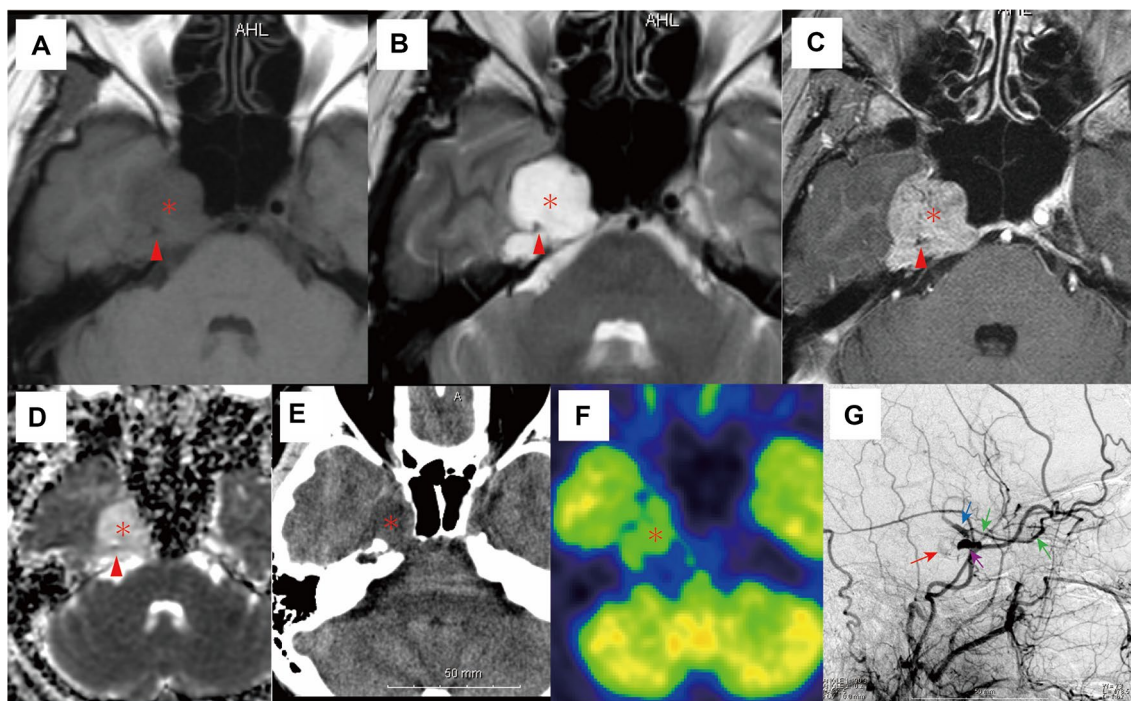

Fig. 2 A 49-year-old woman with right petro-occpital chondrosarcoma (grade II conventional). The tumor appears as a T1-hypointensity (**A**), T2-hyperintensity (**B**) mass with avid homogenous enhancement (**C**). The apparent diffusion coefficient value is high at 1865×10^{-6} mm^2/s (**D**). The tumor has no calcifications (**E**). Positron emission tomography demonstrates that the tumor is mildly colder than the normal brain tissues (**F**), with the lesion-to-normal tissue ratio being 0.65. Right carotid angiogram is performed to examine the patency of the right carotid artery, which demonstrates its complete occlusion, with its distal part (blue arrow) patent through a retrograde collateral from the right ophthalmic artery (green arrow). Notably the cavernous portion of the internal carotid artery (purple arrow) is also patent, and there is faint tumor stain (red arrow) via the inferolateral trunk (**G**, lateral view). Red asterisk and arrowhead indicate the tumor and a remnant of the occluded right internal carotid artery, respectively
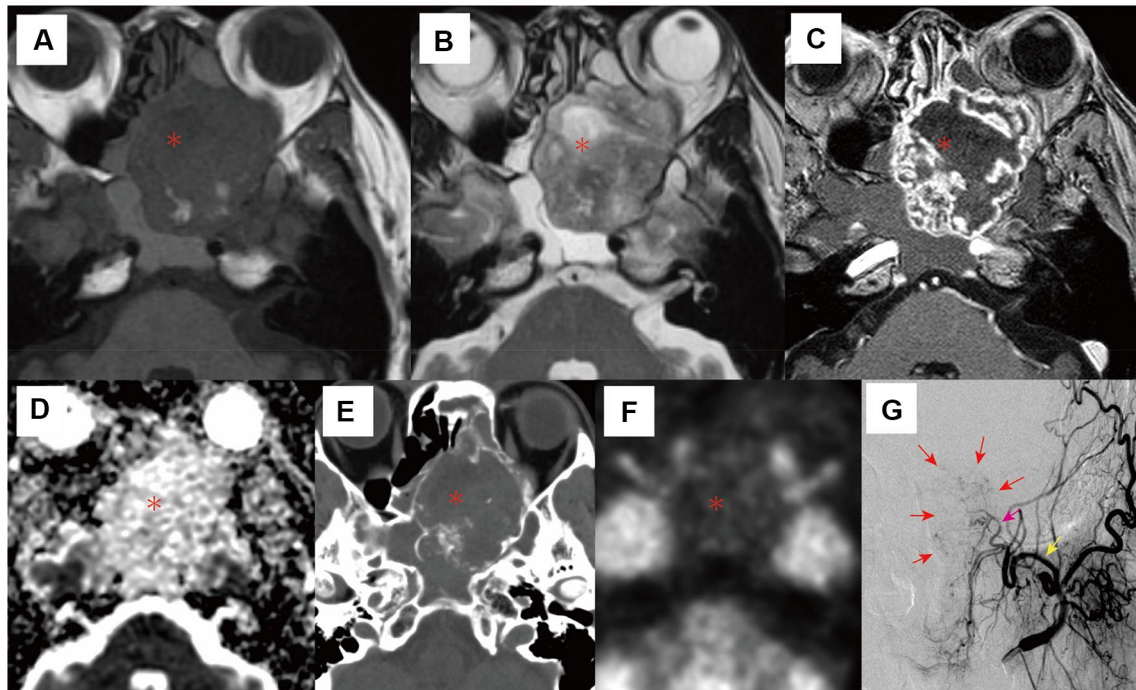
Fig. 3 A 56-year-old man with spheno-ethmoidal chondrosarcoma (grade I conventional). The tumor appears as a T1-hypointensity (**A**), T2-mixed intensity (**B**) mass with "arabesque"-like avid enhancement (**C**). The apparent diffusion coefficient value is high at 2326×10^{-6} mm^2/s (**D**). There are tumoral calcifications on CT (**E**). Positron emission tomography demonstrates that the tumor is significantly colder than the normal brain tissues (**F**), with the lesion-to-normal tissue ratio being 0.2. Left external carotid angiogram demonstrates visible tumor stain (red arrow) from the left sphenopalatine artery (pink arrow) branching from the left internal maxillary artery (yellow arrow) (**G**, A-P view). Red asterisk indicates the tumor

relatively more common in chordoma, while avid (16, 39.0%) or fair (9, 22.0%) enhancement was also possible.

Data on PET was available in 15 SBC and 21 chordoma patients. In SBCs, the PET L/N ratio was generally low-to-intermediate, with the median value being 0.36 (interquartile range, 0.25–0.50). No significant differences in the presence of tumoral calcifications or the PET L/N ratio were observed between SBCs and chordomas (Table 1).

Tumor location

A midline mass without significant laterality was a predominant feature of chordoma (37, 90.2%), while it was also observed in some SBCs (6, 14.6%; P < 0.01). The origins of the SBCs were presumed to be the petro-occipital (27, 65.9%),, spheno-petrosal (5, 12.2%), spheno-ethmoidal (3, 7.3%), pterygo-sphenoidal (2, 4.9%), and spheno-occipital (2, 4.9%) synchondroses. There were two patients in whom SBCs arose from an atypical lateral region (one intraorbital and one lateral petrous). A summary of the tumor locations according to presumed tumor origin is illustrated in Fig. 4.

Factors predictive of a diagnosis of SBC

Bivariate logistic regression analysis demonstrated that the T1SI-ratio (odds ratio [OR] 0.12; 95% confidence interval [CI] 1.39×10^{-2}–0.96; P = 0.04), T2SI-ratio (OR 3.93; 95% CI 1.65–9.40; P < 0.01), ADC value (OR 1.01; 95% CI 1.01–1.02; P < 0.01), little enhancement (OR 0.17, 95% CI 5.04×10^{-2}–0.57, P < 0.01), and non-midline location (OR 54.0, 5% CI 14.0–2.07×10^2, P < 0.01) were significantly associated with an SBC diagnosis. Among them, only ADC value (OR 1.01; 95% CI 1.00–1.02; P < 0.01) remained significant in the multivariate analysis (Table 2).

ROC analysis was performed to further evaluate the association between SBC diagnosis and ADC value. The area under the curve was 0.99, and 1750×10^{-6} mm^2/s was found to maximize the Youden index, which was considered the best cutoff value (Fig. 5). An ADC value of $\geq 1750 \times 10^{-6}$ mm^2/s in fact had a strong association with an SBC diagnosis (OR 5.89×10^2; 95% CI 51.0–6.80×10^3; P < 0.01), yielding a sensitivity of 93.9%, specificity of 97.4%, positive predictive value of 96.9%, and negative predictive value of 95.0%.

Table 1 Summary of the clinical and radiologic characteristics of the patients

Factor	Value						P value
	All n = 82	% or IQR	SBC n = 41	% or IQR	Chor n = 41	% or IQR	
Male sex	35	42.7%	15	36.6%	20	48.8%	0.27
Age at presentation, years	42.5	31.0–59.3	41.0	30.5–54.0	48.0	33.5–61.0	0.24
Presenting symptoms*,**							
CN 2	6	7.3%	3	7.3%	3	7.3%	1.00
CN 3/4/6	41	50.0%	21	51.2%	20	48.8%	1.00
CN 5	6	7.3%	3	7.3%	3	7.3%	1.00
CN 7	2	2.4%	1	2.4%	1	2.4%	1.00
CN 8	2	2.4%	2	4.9%	0	0%	0.49
CN 9/10/11	10	12.2%	4	9.8%	6	14.6%	0.74
CN 12	6	7.3%	2	4.9%	4	9.8%	0.68
Headache/neck pain	8	9.8%	6	14.6%	2	4.9%	0.26
Vertigo	2	2.4%	2	4.9%	0	0%	0.49
Imbalance/gait disturbance	5	6.1%	2	4.9%	3	7.3%	1.00
Exophthalmos	2	2.4%	2	4.9%	0	0%	0.49
Nasal obstruction	3	3.7%	1	2.4%	2	4.9%	1.00
Hypolacrimation	1	1.2%	1	2.4%	0	0%	1.00
Weakness/hemiparesis	2	2.4%	0	0%	2	4.9%	0.49
Otitis media	1	1.2%	0	0%	1	2.6%	1.00
Epistaxis	2	2.4%	1	2.4%	1	2.6%	1.00
Incidental	14	17.1%	5	12.2%	9	22.0%	0.38
Unknown	1	1.2%	1	2.4%	0	0%	/
Radiologic features							
Tumor volume, mL	11.6	7.08–29.4	11.3	7.17–20.9	18.3	6.5–37.1	0.25
T1SI-ratio	0.74	0.57–0.90	0.70	0.53–0.86	0.75	0.59–1.00	0.07
T2SI-ratio	2.20	1.67–2.60	2.39	1.74–2.92	2.01	1.65–2.28	< 0.01
ADC value[†], $\times 10^{-6}$ mm^2/s	1698	1306–2051	2065	1951–2233	1329	996–1521	< 0.01
Tumoral calcification	55	67.9%	30	73.2%	25	62.5%	0.35
PET L/N ratio[‡]	0.41	0.25–0.51	0.36	0.25–0.50	0.43	0.25–0.53	0.66

Data is provided as either number with % or median with IQR

ADC apparent diffusion coefficient, *Chor* chordoma, *CN* cranial nerve, *IQR* interquartile range, *L/N* lesion to normal tissue, *PET* positron-emission tomography, *SBC* skull base chondrosarcoma, *T1SI* T1 signal intensity, *T2SI* T2 signal intensity

*CN 2 includes any patterns of deteriorated vision and visual acuity, CN 3/4/6 includes diplopia and ptosis, CN 5 includes facial sensory disturbance and facial pain, CN 7 includes facial palsy, CN 8 includes vertigo and hearing loss, CN 9/10 includes dysphagia, hoarseness, and weakness of elevation of the shoulder, and CN 12 includes tongue deviation and paralysis of the tongue

**Overlaps exist

[†]Data on ADC value was available in 32 SBC patients and 39 chordoma patients

[‡]Data on PET L/N ratio was available in 15 SBC patients and 21 chordoma patients

Radiologic parameters according to the histological subtypes

The radiologic parameters according to the histological subtypes of SBCs are summarized in Table 3. Between grade I and II SBCs, no significant differences were observed in tumor volume (P = 0.42), midline location (P = 0.55), T1SI-ratio (P = 0.77), T2SI-ratio (P = 0.06), ADC value (P = 0.27), and presence of tumoral calcification (P = 1.00); whereas PET L/N ratio was significantly higher in grade II than in grade I SBCs (P = 0.04).

As for chordomas, there were no statistical differences between conventional and chondroid chordomas in the radiologic parameters except that tumor volume was significantly larger in chondroid chordomas (P = 0.04). The T2SI-ratio of dedifferentiated chordoma appeared to be lower than that of conventional and chondroid chordomas,
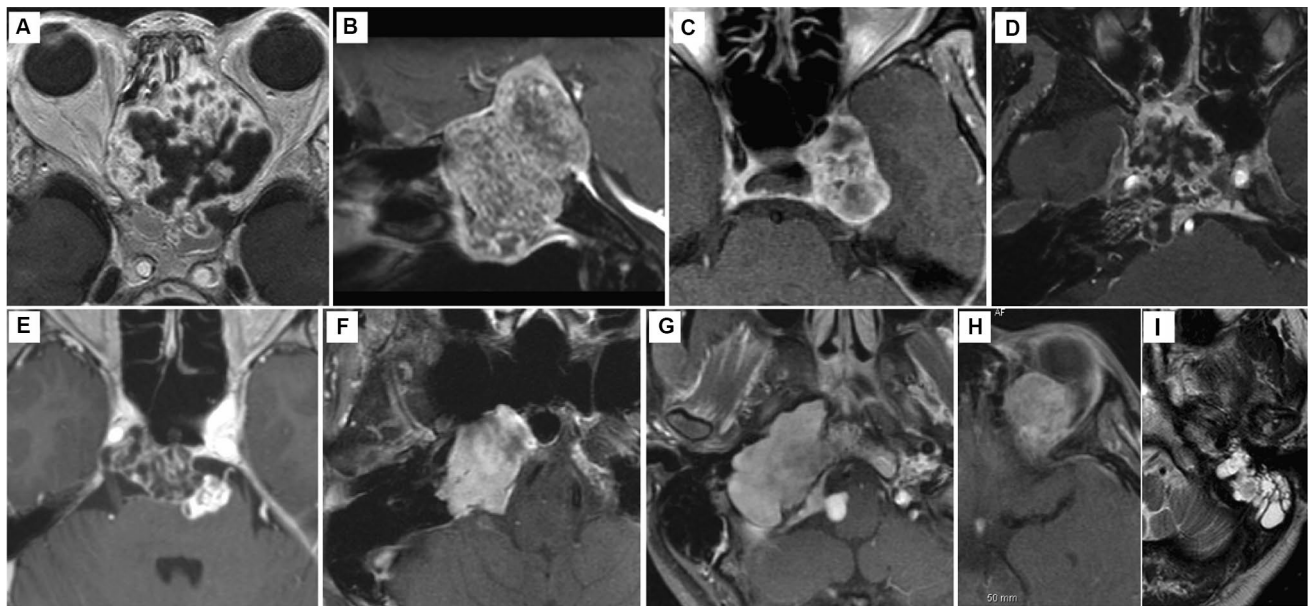
Fig. 4 Representative figures of chondrosarcoma arising from each synchondrosis are shown: **A** spheno-ethmoid; **B** spheno-occipital; **C** Spheno-petrosal; **D** pterygo-sphenoidal; **E** petro-occipital (rostral side, extending in the cavernous sinus); **F** petro-occipital (middle level, centered in the petrous apex); **G** petro-occipital (caudal side, extending in the jugular foramen); **H** intraorbital; **I** lateral petrous

Table 2 Bi- and Multi-variate logistic regression analysis for factors associated with a diagnosis of SBC

Factor	Bivariate			Multivariate		
	OR	95% CI	P value	OR	95% CI	P value
Female sex	1.65	0.68–3.99	0.26	–	–	–
Age at presentation, years	0.99	0.96–1.01	0.22	–	–	–
Headache/neck pain at presentation	3.34	0.63–17.7	0.13	–	–	–
Tumor volume, mL	0.98	0.95–1.00	0.06	–	–	–
T1SI-ratio	0.12	1.39×10^{-2}–0.96	0.04	70.5	3.70×10^{-2}–1.34×10^5	0.25
T2SI-ratio	3.67	1.56–8.63	<0.01	3.21	0.12–86.7	0.50
ADC value*	1.01	1.01–1.02	<0.01	1.01	1.00–1.02	<0.01
Little enhancement	0.17	5.04×10^{-2}–0.57	<0.01	0.32	1.03×10^{-3}–97.0	0.70
Non-midline location	54.0	14.0–2.07×10^2	<0.01	12.8	0.80–2.05×10^2	0.06
Presence of calcifications	1.64	0.64–4.20	0.30	–	–	–
PET L/N ratio**	0.34	6.49×10^{-3}–18.1	0.59	–	–	–

The odds ratios for continuous variables (age, tumor volume, T1SI- and T2SI-ratios, ADC value, and PET L/N ratio) are unit odds ratios

ADC apparent diffusion coefficient, *CI* confidence interval, *OR* odds ratio, *L/N* lesion to normal tissue, *PET* positron-emission tomography, *SBC* skull base chondrosarcoma, *T1SI* T1 signal intensity, *T2SI* T2 signal intensity

*Data on ADC values was available in 32 SBC patients and 39 chordoma patients

**Data on PET L/N ratios was available in 15 SBC patients and 21 chordoma patients

though statistical analysis could not be performed because there was only one patient with dedifferentiated chordoma.

When comparing grade I/II SBCs to conventional chordomas, T2SI-ratio (median 2.51 vs. 2.06; P < 0.01) and ADC value (median 2053×10^{-6} mm²/s vs. 1329×10^{-6} mm²/s; P < 0.01) were significantly higher in grade I/II SBCs. When comparing grade I/II SBCs to chondroid chordomas, tumor volume (median, 10.8 mL vs. 29.8 mL; P < 0.01) was significantly smaller, T2SI-ratio (median 2.51 vs. 1.84; P < 0.01) and ADC value (median 2053×10^{-6} mm²/s vs. 1349×10^{-6} mm²/s; P < 0.01) were significantly higher, and tumoral calcification (72.2% vs. 33.3%; P = 0.05) was marginally more common in grade I/II SBCs.
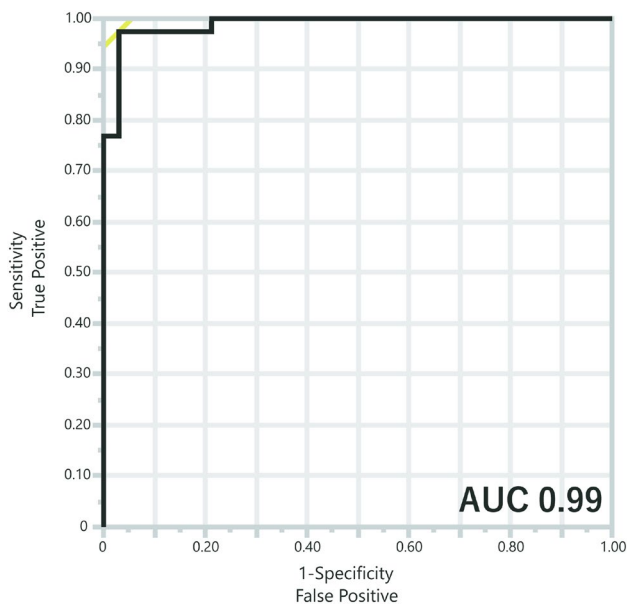
Fig. 5 The receiver-operating curve for the association between the diagnosis of chondrosarcoma and apparent diffusion coefficient value. *AUC* area under the curve

Discussion

The present study depicted the in-depth radiologic features of SBC, in contrast to chordoma. In particular, we found that ADC values were very useful for distinguishing SBCs from chordomas, with the difference in the median values reaching approximately 1.5-fold (2065×10^{-6} mm^2/s vs. 1329×10^{-6} mm^2/s). The multivariate analysis demonstrated that the unit odds ratio for ADC value was 1.01 (1.011596); when using more practical examples, this means that the estimated odds of a tumor being SBC increased by 1.78 or 3.17 for each 50- or 100-point increase in ADC value, respectively. Based on the subtype analyses, the difference in ADC values between SBCs and chordomas was apparently significant regardless of the tumor subtypes. Notably, similar levels of difference in ADC values between SBCs and chordomas were observed in previous studies (2051×10^{-6} mm^2/s vs. 1474×10^{-6} mm^2/s and 2017×10^{-6} mm^2/s vs. 1264×10^{-6} mm^2/s, respectively), suggesting the robustness of this finding [9, 10]. Since ADC value is a measure of the magnitude of water molecule diffusion within tissues, it theoretically reflects the extent of tissue cellularity [10]. Accordingly, ADC value is known to provide a good insight into histological characteristics of the lesions, and can be a good biomarker when distinguishing benign from malignant tumors [22]. Indeed, there are a few previous studies reporting the diagnostic value of diffusion-weighted imaging, which is a secondary product calculated from ADC map [9, 10]. As previously suggested, the difference in ADC values between SBCs and chordomas may possibly result from the difference in their cellularities, structures of extracellular matrices, and/or intracellular components (nuclear-to-cytoplasmic ratio, amount of intracellular proteins, etc.) [10, 23].

Table 3 Summary of the radiologic characteristics according to the histological subtypes

Factor	Chondrosarcoma*					Chordoma		
	Grade I	Grade II	Grade III	Myxoid	Mesenchymal	Conventional	Chondroid	Dedifferentiated
	n = 5	n = 31	n = 2	n = 1	n = 1	n = 30	n = 10	n = 1
Tumor volume, mL	12.7 (8.0–36.0)	10.2 (6.8–21.3)	32.8 (7.9–57.6)	16.3	6.1	11.2 (4.4–34.5)	29.8 (15.2–56.1)	14.1
T1SI-ratio	0.65 (0.52–0.78)	0.67 (0.52–0.88)	0.78 (0.77–0.79)	0.82	0.80	0.75 (0.58–0.99)	0.83 (0.59–1.07)	0.82
T2SI-ratio	2.06 (1.32–2.67)	2.82 (2.19–3.00)	2.04 (1.64–2.45)	2.39	0.96	2.06 (1.67–2.37)	1.84 (1.59–2.01)	1.27
ADC value, $\times 10^{-6}$ mm^2/s	2223 (2053–2326)	2035 (1901–2222)	2105**	2197	No data	1329 (962–1516)	1349 (1129–1646)	1373
Tumoral calcification	4 (80.0%)	22 (71.0%)	2 (100%)	0 (0%)	1 (100%)	4 (80.0%)	4 (80.0%)	1 (100%)
PET L/N ratio‡	0.23 (0.20–0.25)	0.39 (0.31–0.54)	No data	0.25	No data	0.42 (0.21–0.59)	0.44 (0.27–0.50)	No data

Data is provided as either number with % or median with interquartile range

ADC apparent diffusion coefficient, *L/N* lesion to normal tissue, *PET* positron-emission tomography, *T1SI* T1 signal intensity, *T2SI* T2 signal intensity

*One patient with undefined SBC subtype is excluded

**Data on ADC value was available in 1 of 2 grade III chondrosarcoma patients

The key finding of our study is that an ADC value $\geq 1750 \times 10^{-6}$ mm^2/s is highly predictive of SBC diagnosis. Moreover, the diagnostic potential will be further improved if other supportive imaging features of SBC, as detailed below, are considered together. The strength of this prediction method is not only its accuracy, but also its excellent feasibility. Li et al. recently reported a radiomics-based method to distinguish chordoma and SBC with great accuracy [8]. Given the large number of patients and involvement of multiparametric MRI, their method may be more robustly applicable, though this type of method significantly lacks feasibility. However, our method can be readily used in clinical practice, given that ADC values are easy to measure as long as ADC maps are available.

Some MRI findings can support the diagnosis of SBC. Our study confirmed that SBCs exhibit hypointensity to isointensity on T1WI, which is in line with the previous literature [4]. On T2WI, they typically exhibited hyperintensity, which was occasionally mixed with less dominant hypointense areas, likely due to the presence of calcifications. While T2 SI appears to be higher in SBCs than in chordomas, the difference may not be sufficient to be used alone for distinguishing SBC. The majority had fair or avid enhancement. Minimal enhancement was possible, but significantly more likely in chordomas as shown in the univariate analysis. Although arabesque-like enhancement patterns can be seen in some chordomas, they seem to be a hallmark of SBC. This feature, which was previously introduced as "septal or ring-and-arc enhancement" [17, 18], is thought to correspond to fibrovascular bundles surrounding the cartilaginous nodules and is indicative of low-grade SBCs [2]. However, it should be noted that this feature is somewhat subjective and susceptible to an inter-observer error. Although each of the above-mentioned features alone may not be sufficient to support an SBC diagnosis, they will be good markers when combined with the above-mentioned ADC value and tumor volume-based prediction methods.

Regarding the clinical characteristics, including age, sex, and mode of presentation, no significant differences between SBCs and chordomas were observed, although there was a tendency for female predominance in SBCs. Given that mild-to-moderate female predominance has been repeatedly observed in many studies, it appears to be very robust [9, 10, 24–26]. Nevertheless, this predominance alone is not useful to support an SBC diagnosis, since chordoma does not have an apparent sex difference.

Limitations

The present study has several limitations. The retrospective nature and relatively small sample size might have affected the results owing to possible selection bias and underpowered analyses. In addition, our measurements of SIs did not involve the entire volume of the tumor, and thus, the values might be susceptible to intratumoral variability. Especially considering cases of heterogeneous tumors, the measurement of the entire volume might better reflect the characteristics of the tumor. Next, since intratumoral calcification leads to lower ADC values, the present method may not be appropriate for tumors with massive calcification. Moreover, given ADC values may somewhat vary between different MRI machines, the external validity of the present ADC value-based method needs to be further evaluated, and some modifications may be required in the future. Lastly, since the numbers of high grade tumors were limited in our cohort, our result should be cautiously applied when high grade tumors are expected based on their clinical courses. Despite the fact that, in our cohort, the grade III chondrosarcoma exhibited as high an ADC value as the less aggressive subtypes while the dedifferentiated chordoma exhibited as low an ADC value as the less aggressive subtypes, further case accumulation is needed to reach a more robust conclusion. Despite these limitations, our study included one of the largest numbers of patients with "primary" SBC who did not lose the clinical/radiologic features at initial manifestation and thus were the most suitable for examining presurgical diagnosis methods. In addition, the entire volume measurement of SIs and ADC values would be unrealistic in daily clinical practice, and our method has certain advantages in feasibility.

Conclusion

The ADC value appears to be a promising tool to distinguish SBC from chordoma, and an ADC value of $\geq 1750 \times 10^{-6}$ mm^2/s may be an optimal cutoff. The prediction accuracy increases when other features of SBC, such as non-midline location and arabesque-like enhancement, are considered together.

Declarations

Conflict of interest The authors have no relevant financial or non-financial interests to disclose.

Ethical approval The study was approved by Institutional Review board (IRB #2231).

Consent to participate Informed consent was obtained from all individual participants included in the study.

Consent to publish The manuscript does not contain any forms of information on individual details, images or videos.

References

1. Evans HL, Ayala AG, Romsdahl MM (1977) Prognostic factors in chondrosarcoma of bone: a clinicopathologic analysis with emphasis on histologic grading. Cancer 40:818–831
2. Dass AN, Peh WCG, Shek TWH, Ho WK (2008) Case 139: nasal septum low-grade chondrosarcoma. Radiology 249:714–717. https://doi.org/10.1148/radiol.2492040409
3. Rassekh CH, Nuss DW, Kapadia SB, Curtin HD, Weissman JL, Janecka IP (1996) Chondrosarcoma of the nasal septum: skull base imaging and clinicopathologic correlation. Otolaryngol Head Neck Surg 115:29–37. https://doi.org/10.1016/S0194-5998(96)70132-8
4. Meyers SP, Hirsch WL Jr, Curtin HD, Barnes L, Sekhar LN, Sen C (1992) Chondrosarcomas of the skull base: MR imaging features. Radiology 184:103–108. https://doi.org/10.1148/radiology.184.1.1609064
5. Awad M, Gogos AJ, Kaye AH (2016) Skull base chondrosarcoma. J Clin Neurosci 24:1–5. https://doi.org/10.1016/j.jocn.2015.10.029
6. Olson JT, Wenger DE, Rose PS, Petersen IA, Broski SM (2021) Chordoma: (18)F-FDG PET/CT and MRI imaging features. Skeletal Radiol 50:1657–1666. https://doi.org/10.1007/s00256-021-03723-w
7. Doucet V, Peretti-Viton P, Figarella-Branger D, Manera L, Salamon G (1997) MRI of intracranial chordomas. Extent of tumour and contrast enhancement: criteria for differential diagnosis. Neuroradiology 39:571–576. https://doi.org/10.1007/s002340050469
8. Li L, Wang K, Ma X, Liu Z, Wang S, Du J, Tian K, Zhou X, Wei W, Sun K, Lin Y, Wu Z, Tian J (2019) Radiomic analysis of multiparametric magnetic resonance imaging for differentiating skull base chordoma and chondrosarcoma. Eur J Radiol 118:81–87. https://doi.org/10.1016/j.ejrad.2019.07.006
9. Muller U, Kubik-Huch RA, Ares C, Hug EB, Low R, Valavanis A, Ahlhelm FJ (2016) Is there a role for conventional MRI and MR diffusion-weighted imaging for distinction of skull base chordoma and chondrosarcoma? Acta Radiol 57:225–232. https://doi.org/10.1177/0284185115574156
10. Yeom KW, Lober RM, Mobley BC, Harsh G, Vogel H, Allagio R, Pearson M, Edwards MS, Fischbein NJ (2013) Diffusion-weighted MRI: distinction of skull base chordoma from chondrosarcoma. AJNR Am J Neuroradiol 34(1056–1061):S1051. https://doi.org/10.3174/ajnr.A3333
11. Weber DC, Malyapa R, Albertini F, Bolsi A, Kliebsch U, Walser M, Pica A, Combescure C, Lomax AJ, Schneider R (2016) Long term outcomes of patients with skull-base low-grade chondrosarcoma and chordoma patients treated with pencil beam scanning proton therapy. Radiother Oncol. https://doi.org/10.1016/j.radonc.2016.05.011
12. Bohman LE, Koch M, Bailey RL, Alonso-Basanta M, Lee JY (2014) Skull base chordoma and chondrosarcoma: influence of clinical and demographic factors on prognosis: a SEER analysis. World Neurosurg 82:806–814. https://doi.org/10.1016/j.wneu.2014.07.005
13. Wang L, Wu Z, Tian K, Wang K, Li D, Ma J, Jia G, Zhang L, Zhang J (2017) Clinical features and surgical outcomes of patients with skull base chordoma: a retrospective analysis of 238 patients. J Neurosurg 127:1257–1267. https://doi.org/10.3171/2016.9.JNS16559
14. Hasegawa H, Vakharia K, Graffeo CS, Carlson ML, Pollock BE, Brown PD, Perry A, Van Gompel JJ, Driscoll CLW, Link MJ (2021) Long-term outcomes of grade I/II skull base chondrosarcoma: an insight into the role of surgery and upfront radiotherapy. J Neurooncol 153:273–281. https://doi.org/10.1007/s11060-021-03764-0
15. Shinya Y, Hasegawa H, Shin M, Kawashima M, Koga T, Hanakita S, Katano A, Sugiyama T, Nozawa Y, Saito N (2022) High dose radiosurgery targeting the primary tumor sites contributes to survival in patients with skull base chordoma. Int J Radiat Oncol Biol Phys 113:582–587. https://doi.org/10.1016/j.ijrobp.2022.02.024
16. Vandenbroucke JP, von Elm E, Altman DG, Gotzsche PC, Mulrow CD, Pocock SJ, Poole C, Schlesselman JJ, Egger M, S initiative (2007) Strengthening the Reporting of Observational Studies in Epidemiology (STROBE): explanation and elaboration. Ann Intern Med 147:W163-194. https://doi.org/10.7326/0003-4819-147-8-200710160-00010-w1
17. Famuyide A, Juliano A, Moonis G (2021) MRI of sinonasal malignancies. Top Magn Reson Imaging 30:139–149. https://doi.org/10.1097/RMR.0000000000000288
18. De Beuckeleer LHL, De Schepper AMA, Ramon F, Somville J (1995) Magnetic resonance imaging of cartilaginous tumors: a retrospective study of 79 patients. Eur J Radiol 21:34–40. https://doi.org/10.1016/0720-048x(96)81067-9
19. Kothari RU, Brott T, Broderick JP, Barsan WG, Sauerbeck LR, Zuccarello M, Khoury J (1996) The ABCs of measuring intracerebral hemorrhage volumes. Stroke 27:1304–1305. https://doi.org/10.1161/01.str.27.8.1304
20. Hirata K, Tamaki N (2021) Quantitative FDG PET assessment for oncology therapy. Cancers 13:869. https://doi.org/10.3390/cancers13040869
21. Youden WJ (1950) Index for rating diagnostic tests. Cancer 3:32–35. https://doi.org/10.1002/1097-0142(1950)3:1%3c32::aid-cncr2820030106%3e3.0.co;2-3
22. Sun Y, Tong T, Cai S, Bi R, Xin C, Gu Y (2014) Apparent diffusion coefficient (ADC) value: a potential imaging biomarker that reflects the biological features of rectal cancer. PLoS ONE 9:e109371. https://doi.org/10.1371/journal.pone.0109371
23. Filippi CG, Edgar MA, Ulug AM, Prowda JC, Heier LA, Zimmerman RD (2001) Appearance of meningiomas on diffusion-weighted images: correlating diffusion constants with histopathologic findings. AJNR Am J Neuroradiol 22:65–72
24. Dibas M, Doheim MF, Ghozy S, Ros MH, El-Helw GO, Reda A (2020) Incidence and survival rates and trends of skull Base chondrosarcoma: a Population-Based study. Clin Neurol Neurosurg 198:106153. https://doi.org/10.1016/j.clineuro.2020.106153
25. Raza SM, Gidley PW, Kupferman ME, Hanna EY, Su SY, DeMonte F (2018) Site-specific considerations in the surgical management of skull base chondrosarcomas. Oper Neurosurg 14:611–619. https://doi.org/10.1093/ons/opx171
26. Holtzman AL, Rotondo RL, Rutenberg MS, Indelicato DJ, Mercado CE, Rao D, Tavanaiepour D, Morris CG, Louis D, Flampouri S, Mendenhall WM (2019) Proton therapy for skull-base chondrosarcoma, a single-institution outcomes study. J Neurooncol 142:557–563. https://doi.org/10.1007/s11060-019-03129-8